ISSN 1590-8844
International Journal of Mechanics and Control, Vol. 20, No. 01, 2019

ANALYSIS OF SERIES ELASTICITY IN LOCOMOTION OF A PLANAR BIPEDAL ROBOT

Silvia Manara[*] Gian Maria Gasparri[**] Manolo Garabini[**] Danilo Caporale[**]
Marco Gabiccini[*] Antonio Bicchi[**]

[*] Dipartimento di Ingegneria Civile e Industriale, Università di Pisa, Italy

[**] Centro di Ricerca "E. Piaggio", Università di Pisa, Italy

ABSTRACT

The great promise of series elastic actuation as an effective mean to improve the efficiency of dynamic bipedal locomotion is challenged by the difficulties in properly exploiting the dynamics of the system, due to the mutual influence between inputs and stiffness of the elastic elements. Although numerical optimisation has proven to be a valid tool to approach this problem, the contexts in which the energy improvement justifies the greater design effort are not clear yet. To fill this gap, this work presents an extensive numerical study in which optimised walking and running gaits are compared for a planar bipedal robot, driven either by rigid or series elastic actuators, whose stiffness is selected concurrently with the input trajectories. The comparison shows that: *i*) the Cost of Transport relative to the soft robot with optimised stiffness is lower than that obtained for its rigid counterpart, especially in running; *ii*) the forward speed for which running is more efficient than walking is lower for the soft robot than for its rigid counterpart; *iii*) the soft robot with optimised stiffness can run significantly faster than its rigid counterpart.

Keywords: Soft Robotics, Series Elasticity, Locomotion, Optimal Control.

1 INTRODUCTION

Taking inspiration from nature, Soft Robotics (SR) aims to build machines whose compliant physical structure is able to mimic the characteristics of biologic actuation [1]. Two main branches exist in SR. The first one, inspired by invertebrate animals, focuses on robots whose compliance is distributed in the whole structure, made of continuously flexible materials [2]. The other branch, inspired by the musculoskeletal system of vertebrates, instead, concentrates on robots whose compliance is mostly concentrated in the joints, driven by compliant actuators [3]. Robots of this kind are also referred to as articulated soft robots, or elastic-joint robots.

Contact author: Silvia Manara
Dipartimento di Ingegneria Civile e Industriale, Largo Lucio Lazzarino 1, 56122 Pisa, Italy
E-mail: silviamanara1@gmail.com

Elastic-joint robots have proven to be energetically more efficient than their rigid counterparts, due to their ability to store and release elastic energy, see e.g. [4, 5]. This feature is expected to be particularly beneficial for robotic locomotion: one of the key factors of the efficiency of human locomotion, in fact, is the compliant actuation characterising the musculoskeletal system [6, 7]. Studies on simplified models have confirmed such expectation [8, 9]. These results, obtained for systems with few (one or two) degrees of freedom (DoF), suggest that SR provides new opportunities for enhancing the energy efficiency of robotic locomotion. Thus, several complex soft robots have been realised. Remarkable examples of soft humanoid robots are, e.g., Walk-Man [10], ESCHER [11], DURUS [12]. However, compared to rigid robots, the presence of compliant elements increases the complexity of the control synthesis [13]. This is due to several factors, such as the increased state size and degree of underactuation, or the mutual influence between the stiffness of the elastic elements and the input trajectories. The synthesis of bipedal gaits has traditionally attracted significant interest in the scientific community. A common

approach, explored on simplified models [14], takes advantage of the application of Numerical Optimal Control (NOC). Recently, considerable efforts have been devoted to extending such results to increasingly complex systems. For instance, NOC was employed in [15] to optimise a running motion of a human-like biped, where the joint elasticity was introduced by passive elastic elements acting in parallel with the actuators, rather than by Series Elastic Actuators (SEAs). In [16], a 6-DoF bipedal model was considered where the compliance was concentrated only at the ankles, driven by parallel elastic actuators. Both the ankle stiffness and the gait parameters were determined through the optimisation of energy efficiency. In [17], a direct optimal control method was applied to the optimisation of walking gaits for a 6-DoF planar robot actuated via SEAs. However, the actuator compliance was not designed to optimise the efficiency of motion.

In the present paper, state-of-the-art modelling [18] and optimisation [19, 20] tools are employed to simultaneously determine stiffness and motor position references of a 6-DoF planar biped with elastic joints, by minimising the energy expenditure in both walking and running. The main goal is to gain further insight into the influence of series elasticity in locomotion of complex elastic-joint bipeds. To this aim, the performance of optimal walking and running gaits of a robot actuated via SEAs is compared to that of a rigidly actuated model. The sensitivity of energy efficiency of locomotion to stride parameters, i.e. forward speed and clearance of the floating foot, is assessed through extensive numerical tests. In a recent contribution [21], NOC was applied to the optimal design of walking gaits for several biped models of increasing complexity, driven either by parallel or series elastic actuators. Compared to the analysis proposed in that paper, this work presents an extensive analysis on a wider range of stride characteristics. Indeed, both walking and running gaits are investigated here, in order to establish in which range of application SEAs are particularly effective in improving the energy efficiency of locomotion. A similar energetic performance analysis was presented in [22] for the bipedal robot ATRIAS: therein, the energy expenditure of walking gaits over a given interval of average forward speed was assessed. In [23], instead, NOC was applied to synthesise different kind of gaits for two simple robotic models: a biped and a quadruped, both planar and actuated by SEAs. Specifically, the energetic trade-off between walking and running was assessed for the bipedal model. Similarly, the numerical results presented in this paper allow a quantitative assessment of the energetic efficiency of locomotion for the investigated robot model. Our findings are consistent with those presented in the aforementioned previous studies.

The paper is structured as follows. In Section 2, the dynamics of both the rigid and the soft model are described and the gait optimisation problem is introduced. In Section 3, after a brief description of the characteristics of the robot used as a case study, the optimisation results are presented and analysed. Finally, concluding remarks are drawn in Section 4.

2 PROBLEM STATEMENT

Walking and running gaits are obtained through nonlinear programming (and therefore guaranteed to be at least locally optimal) for two models describing the same planar biped robot, powered by two different kind of actuators: rigid and series elastic, respectively. For both models, the dynamic equations were efficiently generated using the software Robotran [18].

2.1 RIGID MODEL

Let n_a denote the number actuated internal joints of the robot and $\chi \in \mathbb{R}^{n_a}$ the vector collecting the positions of the respective internal joint angles. Similarly, let n_d denote the number of degrees of freedom of the floating base (which is 3, since the robot is planar) and $\chi_f \in \mathbb{R}^{n_d}$ the vector describing the pose of the floating base in the plane, i.e. $\chi_f = (p_y, p_z, \phi)^\top$, ϕ being the orientation of the trunk and p_y, p_z the Cartesian coordinates of the position of its center of mass. The configuration of the robot can be parametrised by $q = (\chi, \chi_f)^\top \in \mathbb{R}^{n_a+n_d}$. Then, the dynamics of the rigid biped reads

$$M_R(q)\ddot{q} + C_R(q,\dot{q})\dot{q} + B_R\dot{q} + G(q) = \sum_{i=1}^{n_p} J_i(q)^\top w_i + \tau_R(u) \quad (1)$$

where $M_R(q)$ represents the robot inertia matrix and $G(q)$ the gravitational term. The term $C_R(q,\dot{q})\dot{q}$ accounts for the Coriolis and centrifugal contributions. In order to obtain comparable results, the rigid actuators were assumed to have the same damping and inertial properties as the SEAs. As such, the damping matrix B_R can be expressed as

$$B_R = \begin{bmatrix} B & 0_{n_a \times n_d} \\ 0_{n_d \times n_a} & 0_{n_d \times n_d} \end{bmatrix} \quad (2)$$

where $B = \mathrm{diag}(b)$, $b \in \mathbb{R}^{n_a}$ being the vector of motor damping. Furthermore, since in this case the motor output shaft rotates rigidly with the link of the robot to which it is connected, its rotational inertia is added to that of the link. $w_i \in \mathbb{R}^{n_d}$ is the external wrench acting on the i-th support foot at the contact point p_i, whose Jacobian is $J_i(q)$. n_p represents the current number of feet that are in contact with the ground and $\tau_R(u) \in \mathbb{R}^{n_a+n_d}$ is the vector of generalized forces, whose components coincide with those of the vector of motor torques $u \in \mathbb{R}^{n_a}$ in case the corresponding DoF is actuated and are zero otherwise (i.e. for the 3 DoF of the floating base).

2.2 SOFT MODEL

When SEAs are employed, the motor torques u do not act directly on the links of the robot, as in the rigidly actuated

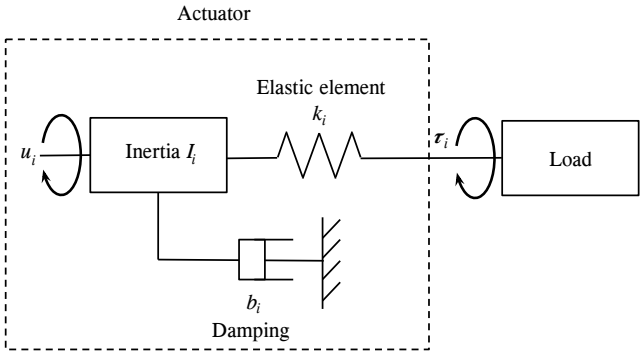

Figure 1 Schematic of a Series Elastic Actuator (SEA).

case. They are rather applied to the links of the robot through elastic elements, which are placed between each motor and the relative output shaft [24]. The dynamics of the system is therefore coupled with that of the motors. The schematic of a SEA can be found in Figure 1. As proposed in [25], the gyroscopic interactions between the motors and the links are neglected, such that the model of the soft biped results in the following system of $n_d + 2n_a$ equations

$$\begin{cases} M_S(q)\ddot{q} + C_S(q,\dot{q})\dot{q} + G(q) = \sum_{i=1}^{n_p} J_i(q)^\top w_i + \tau_S(\delta,k) \\ I\ddot{\theta} + B\dot{\theta} + K\delta = u \end{cases} \tag{3}$$

Here, $\theta \in \mathbb{R}^{n_a}$ represents the motor positions, $\delta = \theta - \chi$ the vector collecting the deflection angles of all the motors, i.e. the difference between each motor angle and the angular position of the corresponding link. $M_S(q)$ is the inertia matrix and $C_S(q,\dot{q})\dot{q}$ takes into account the Coriolis and centrifugal effects. It is worth highlighting that, unlike $M_R(q)$ and $C_R(q,\dot{q})$, the rotational inertia of the motor is not taken into account in $M_S(q)$ and $C_S(q,\dot{q})$. I and B are the motor inertia and damping matrices, respectively. In order to effectively exploit the dynamics of the system, the vector of joint stiffness $k \in \mathbb{R}^{n_a}$ is included among the optimisation variables, and it is assumed to be constant over time, as we aim to investigate series elastic actuation. $K = \mathrm{diag}(k)$ is the motor stiffness matrix and $\tau_S(\delta,k) \in \mathbb{R}^{n_a+n_d}$ is the vector of generalized forces, whose components coincide with those of $K\delta$ in case the corresponding DoF is actuated and are zero otherwise.

2.3 CONTACT PHASES

A multi-phase formulation is employed to describe the dynamics of the robot through the different contact phases, whose sequence is *a priori* prescribed. Specifically, in the optimisation of walking gaits an alternation of single- and double-support phases is imposed, whereas in the optimisation of running motions the single-support phases are alternated with flight phases, where none of the feet is in contact with the ground (see Figure 2). During contact

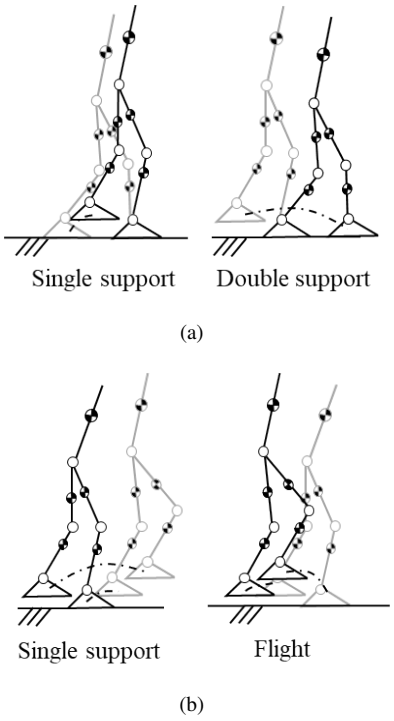

Figure 2 Schematic of the 6-DoF biped used in the optimisations (a) walking and (b) running.

phases in which at least one foot is in contact with the ground, i.e. $n_p \geq 1$, neither sliding nor interpenetration between each support foot and the ground are allowed. The contact model is thus captured by holonomic constraints on the position of the support feet, which must be properly taken into account in the dynamics, through the equations

$$J(q)\ddot{q} = \gamma(q,\dot{q}) \tag{4a}$$

$$\mathfrak{I}(q,\dot{q}) = \begin{pmatrix} c(q) \\ J(q)\dot{q} \end{pmatrix} = 0 \tag{4b}$$

where $c(q)$ represents the holonomic constraints, $J(q) = \partial c(q)/\partial q$ and $\gamma(q,\dot{q}) = -((\partial J(q)/\partial q)\dot{q})\dot{q}$. (4b) are invariants on position and velocity level, that are referred to as $\mathfrak{I}$. The dynamics of the system during each contact phase is obtained by jointly imposing (1) and (4) in the rigid case, and (3) and (4) in the soft case.

The transition between two subsequent contact phases occurs when a foot impacts the ground. The impact is assumed to be fully inelastic and without sliding. The relation describing the velocity discontinuity due to the impact of the i-th contact foot reads

$$\begin{cases} M(q)(\dot{q}^+ - \dot{q}^-) = J_i(q)^\top \tilde{w} \\ J_i(q)\dot{q}^+ = 0 \end{cases} \tag{5}$$

where $\tilde{w} \in \mathbb{R}^3$ is a vector representing the impulsive contact wrench and, in order to simplify the notation, $\dot{q}^-$

and $\dot{q}^+$ respectively indicate $\dot{q}(t_s^-)$ and $\dot{q}(t_s^+)$, i.e. the velocities immediately preceding and immediately following the impact with the ground occurring at time t_s. The parameter t_s is included among the optimisation variables, such that the set of parameters to be optimised are $p = \{t_s, \tilde{w}\}$ in the rigid case and $p = \{t_s, \tilde{w}, k\}$ in the soft case. All the other states are continuous through the phase change [26].

2.4 PERIODICITY

Only gaits that are symmetric with respect to the sagittal plane of the system are considered here. Therefore, only half of a gait cycle is optimised. Let T indicate the gait period. We optimise over the time interval $t \in [0, T_h]$ with $T_h = \frac{T}{2}$, assuming that the entire cycle can be obtained with a switch of states and controls between left and right side of the system at time T_h. It should be noted that in the optimisation of soft gaits, the stiffness of each actuator is constrained to be equal to the stiffness of the corresponding joint on the opposite leg, such that no discontinuity in the joint stiffness occurs when the two legs switch their roles at $t = T_h$. The motion periodicity is imposed through constraints relating the state of the system at $t = 0$ to the state at $t = T_h$, i.e.

$$x_{\text{red}}(0) = \Pi x_{\text{red}}(T_h) \tag{6}$$

Here, x_{red} is a vector collecting the periodic states, i.e. all the states of the system except for the position p_y of the floating base in the locomotion direction, and Π is a permutation matrix representing the symmetry with respect to the sagittal plane.

2.5 OPTIMAL CONTROL PROBLEM

Given all the previous considerations, the trajectories are synthesised by solving an Optimal Control Problem (OCP), which can be stated in the same general form as

$$\min_{x(\cdot),u(\cdot),w(\cdot),p} \quad \int_0^{T_h} \frac{\|u(t)\|^2}{mgL} dt \tag{7}$$

$$\text{subject to} \quad F_i(x(t), \dot{x}(t), w(t), u(t), p) = 0, \qquad i \in \mathscr{C} \tag{8}$$

$$\Delta(x(t_s^+), x(t_s^-), p) = 0, \tag{9}$$

$$Z^\top (x_{\text{red}}(0) - \Pi x_{\text{red}}(T_h)) = 0, \tag{10}$$

$$h(x(t), u(t), w(t), p) \geq 0. \tag{11}$$

Since both the gait period T and the step length L are given, the average speed in the locomotion direction is fixed. This point will be discussed further in Section 3.1. The Cost of Transport (CoT) [27] is optimised in (7), where m denotes the mass of the system and g the gravity acceleration. More in detail, the objective function is a performance index that can be interpreted as a measure of the electrical energy needed to perform the task. In (8), the Equations of Motion are imposed, $F_i(\cdot)$ representing the dynamics of the system during the i-th contact phase. Due to periodicity and symmetry, the set of contact phases is $\mathscr{C} = \{1, 2\}$, where 1 and 2 represent the single- and the double-support phase in the optimisation of a walking gait, or the flight and the single-support phase in the optimisation of a running gait. In (9), the function $\Delta(\cdot)$ describes the state discontinuity at the phase change occurring at time t_s, due to the impact of one foot with the ground. In the optimisation of walking gaits, due to the invariants (4b) in the dynamics, the periodicity constraint needs to be projected into the null-space of the Jacobian of the invariants, in order to avoid redundancies in the constraints, see [28]. Thus, in (10), Z is a basis of the null-space of the Jacobian $\frac{\partial \mathfrak{I}_s}{\partial x_{\text{red}}}\big|_{t=0}$, where $\mathfrak{I}_s$ represents the invariants on position and velocity of the stance foot, that are preserved over the single-support phase and the subsequent double-support phase. In the optimisation of running gaits, instead, this issue does not arise, as in the flight phase no holonomic constraints hold on the position of the feet. Therefore, in this case Z equals the identity matrix.

Additional inequality constraints are given in (11) to guarantee that: *i*) the external contact wrench w belongs to the static friction cone; *ii*) the contact is unilateral, i.e. the normal component of the contact force is non-negative; *iii*) the Center of Pressure (CoP) is inside the support area; *iv*) limits on joint positions and velocities are met; *v*) control saturation is taken into account; *vi*) there is a minimum clearance f_h between each floating foot and the ground. Specifically, the foot has to reach a minimum height within a given time interval, and cannot go below it until it impacts the ground again.

2.6 NUMERICAL SOLUTION

The OCP is solved numerically by employing a direct collocation method [29]. The time horizon is discretised into N time intervals and the state and control trajectories are parametrised by the sequences $\{x_k\}$ and $\{u_k\}$ of optimisation variables, such that the continuous time OCP results in a finite-dimensional nonlinear program (NLP). Specifically, the controls u_k are assumed piece-wise constant over each time interval $[t_k, t_{k+1}]$, whereas the current state x_k is related to the next state x_{k+1} by employing a polynomial interpolation $x(x_k^c, t)$ to approximate the dynamic evolution of the state of the system $x(t)$ over the time interval $[t_k, t_{k+1}]$. The contact wrench $w(t)$ is also approximated via a polynomial approximation denoted as $w(w_k^c, t)$. In order to determine the coefficients x_k^c and w_k^c that identify the interpolation polynomials, the dynamic constraints are imposed at c collocation points per time interval, c being the degree of the interpolating polynomial. Therefore, in accordance with the direct collocation method, the following system of equations is imposed

$$\begin{cases} x(x_k^c, t_k) = x_k \\ F_i(x(x_k^c, t_{k,j}), \frac{\partial x(x_k^c, t)}{\partial t}\big|_{t=t_{k,j}}, w(w_k^c, t_{k,j}), u_k, p) = 0, \\ \qquad\qquad \forall j \in \{1, \ldots, c\} \end{cases} \tag{12}$$

Table I - Values of the physical parameters of the model.

Parameter	Value
Tibia mass	1.00 kg
Femur mass	0.70 kg
Pelvis mass	1.70 kg
Foot mass	0.55 kg
Trunk mass	1.00 kg
Tibia length	0.18 m
Femur length	0.12 m
Pelvis length	0.11 m
Trunk length	0.15 m
Torque limit	± 6 Nm
Motor inertia	$2.33 \cdot 10^{-2}$ kg $\cdot$ m^2
Motor damping	0.08 Nms/rad

with k belonging to the i-th contact phase. It should be noted that the time-derivative $\frac{\partial x(x_k^c,t)}{\partial t}$ of the polynomial $x(x_k^c,t)$ at the j-th collocation point $t = t_{k,j}$ is known in a closed form. By consistently approximating the cost function and the constraints, the OCP results in the following NLP

$$\begin{aligned} \min_{\xi} \quad & f(\xi) \\ \text{subject to} \quad & g(\xi) = 0 \\ & h(\xi) \geq 0 \end{aligned} \tag{13}$$

where $\xi = (x_0, x_0^c, \dot{x}_0^c, w_0^c, u_0, \ldots, x_k, x_k^c, \dot{x}_k^c, w_k^c, u_k, \ldots, x_N, p)^\top$ denotes the vector collecting all the decision variables. The NLP (13) was formulated in the CasADi framework [19] and solved numerically, using the interior-point solver IPOPT [20].

3 CASE STUDY: 6-DoF BIPED

The model and the stride parameters used in the generation of locomotion trajectories are described in Section 3.1. Section 3.2 presents the numerical results.

3.1 MODEL AND TASKS DESCRIPTION

The system considered in this study is a 6-DoF planar biped, composed of a trunk jointed to two legs, having 3 DoF each. The physical parameters of the system are provided in Table I. These parameters were chosen in such a way that the model is representative of the dynamics of the robot *SoftLegs*, depicted in Figure 3. Namely, the robot is a 6-DoF planar biped, driven by *Qbmove Advanced* Variable Stiffness Actuators (VSAs) [30], that are electrically powered and backdrivable. In principle, such actuators are tailored to vary the joint stiffness on-line. However, here we assume to benefit only from their capability to tune the stiffness of the series elastic elements, so as to mimic the dynamics of SEAs, that are the subject of our study. The robot is made of two 3-DoF planar legs, jointed to a pelvis on which a trunk is installed. The ankle joints are driven by a four-bar

Figure 3 The *SoftLegs* robot. The system consists of a trunk (1) and two planar legs (2) having 3 DoF each. An external structure (3) constrains the dynamics of the robot to evolve on its sagittal plane.

mechanism. The end-effector of each leg consists of a flat foot. Two parallel walls made of plexiglass and supported by an external structure constrain the dynamics of the system to evolve on its sagittal plane. In order to reduce the friction between the trunk of the robot and the walls, four spherical bearings are interposed between each couple of adjacent surfaces.

The following relation is employed to link the step length to the locomotion speed:

$$\sigma = \alpha v^\beta \tag{14}$$

where $\sigma = L/l$ is the step length normalized by the leg length l and $v = L/(T_h\sqrt{l/g})$ is the normalized forward speed. Hereinafter, the subscripts w and r denote walking and running, respectively. In case of walking, the scalar parameters α, β were set to $\alpha_w = 1$ and $\beta_w = 0.42$, in accordance with [31], while in case of running $\alpha_r = 1.06$ and $\beta_r = 0.37$ were obtained by interpolating the results provided in [32] at minimum RMSE.

3.2 OPTIMISATION RESULTS

In the following, the results obtained from the numerical optimisation of walking and running gaits, i.e. from the solution of the NLP in (13), are presented and the performance of rigid and soft models are compared.

3.2.1 Actuators: rigid vs. soft

The swing foot clearance f_h was chosen in the interval $f_h \in [0, 0.03]$ m, whereas the parameters T, L were set in accordance with (14), in such a way that the walking speed $v_w \in [0.1, 0.6]$ m/s and the running speed $v_r \in [0.1, 1]$ m/s. Snapshots of two optimised walking and running gaits are shown in Figure 4. In Figure 5, the results obtained in terms of CoT as a function of the considered stride parameters are presented, for the walking case. For both the rigid (Figure 5(a)) and the soft model (Figure 5(b)), the CoT increases as function of the locomotion speed in the considered interval. Moreover, due to the robot inertia distribution, which is highly concentrated in the legs

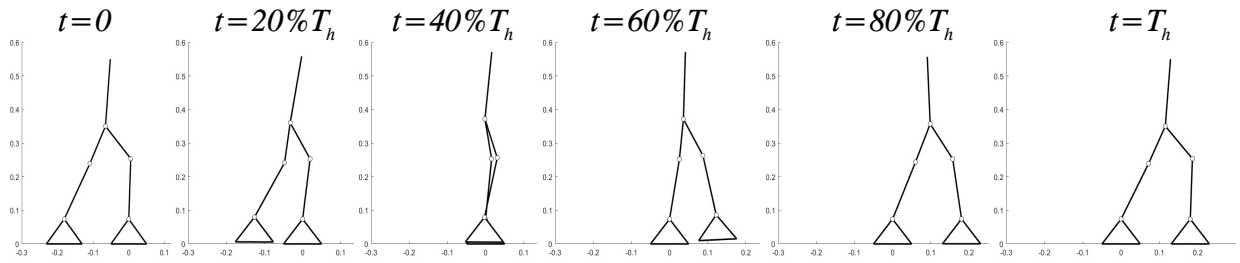

(a)

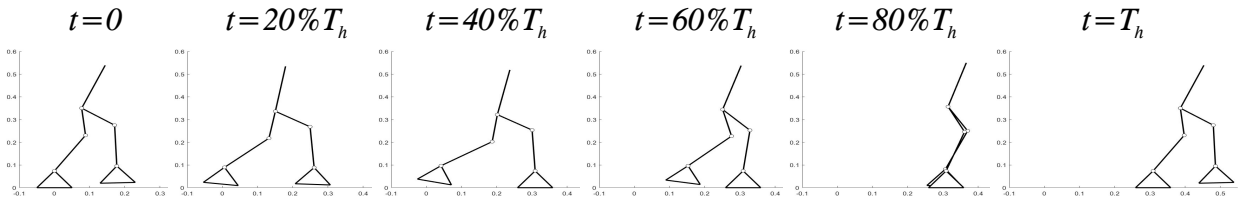

(b)

Figure 4 Visualization of two optimal solutions obtained in case of (a) walking and (b) running.

(specifically, the mass of each leg is 2.25 kg, with the overall mass of the system being 7.2 kg), the CoT increases as f_h increases, especially when the speed is relatively high. For low values of the forward speed, the obtained optimal solution is a compass walk when $f_h = 0$.

Let us now compare the gaits optimised for the two models. Figure 6 shows rigid and soft most efficient solutions, for both walking and running. It is worth noting that the soft model allows for remarkable energy saving compared to the rigid one, especially with regard to running. In case of walking, the rigid model and the soft one present comparable CoTs at low speed, whereas the energy saving becomes more evident as v_w increases.

In case of running with rigid actuators, the OCP, where limits on motor torque and speed are imposed, cannot be solved for several values of forward speed and foot clearance. Indeed, results are obtained just for v_r in a limited subset (see curve labelled as *Rigid Run* in Figure 6). Instead, when SEAs are employed, the inertia decoupling resulting from the introduction of elastic elements between the links and the motors allows the solver to compute optimal solutions for a considerably wider set of values of v_r (see curve *Soft Run* in Figure 6). The soft model outperforms the rigid one in running: the CoT is considerably lower over the whole forward speed range.

Let v_{wr} denote the walk-to-run speed transition, i.e. the speed at which running becomes energetically more convenient than walking. In the rigid case $v_{wr} = 0.44\,\mathrm{m/s}$. In the soft case, instead, a lower transition speed can be observed, i.e. $v_{wr} = 0.38\,\mathrm{m/s}$. Furthermore, a rigid-to-soft speed transition v_{RS}, i.e. a speed at which soft actuation becomes more efficient than rigid actuation, can also be identified: namely, $v_{RS} = 0.15\,\mathrm{m/s}$.

3.2.2 Stiffness analysis

Numerical optimisation results show how a proper exploitation of the compliance of the system can lead to remarkable energy savings. In the following, the obtained stiffness trends are analysed. Specifically, let us focus on the Cartesian stiffness [33] of the stance leg, which can be estimated as

$$K_L(q) = J_L(q)^{\dagger\top} K J_L(q)^{\dagger} \tag{15}$$

where $J_L(q)$ denotes the Jacobian of the contact point and $J_L(q)^{\dagger}$ its pseudoinverse matrix. Due to its dependence on the configuration q of the robot, the Cartesian stiffness K_L varies over the considered time horizon. However, in both walking and running, the eigenvector associated to the maximum eigenvalue of the Cartesian stiffness matrix K_L of the stance leg is directed almost vertically over the whole time horizon. Therefore, the element K_{zz} of the stance-leg stiffness matrix, i.e. the stiffness relative to the vertical direction, was analysed, particularly focusing on its dependence on the locomotion speed. The results of this analysis are presented in Figure 7, for both walking and running. In walking (Figure 7(a)), K_{zz} significantly decreases as the forward speed increases. Qualitatively, these results may be better understood by considering the motion of the stance leg, which is sketched in Figure 8 for different values of the forward speed v_w. The stance leg is straight at low speed. Indeed, as already mentioned, for low values of v_w, the optimal solution is a compass walk when $f_h = 0$. As the forward speed increases, the stance leg configuration changes: the knee is progressively more bent. As a result

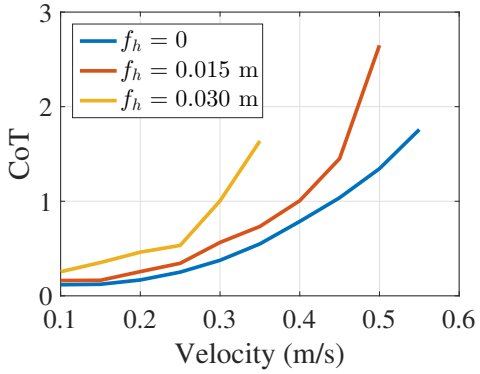

(a)

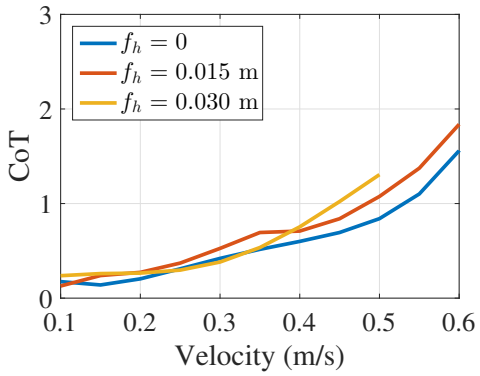

(b)

Figure 5 (a) Rigid Walk CoT trend as a function of the forward speed. (b) Soft Walk CoT trend as a function of the forward speed. In both plots, the curves are identified by the minimum value imposed to the clearance of the swing foot from the ground f_h.

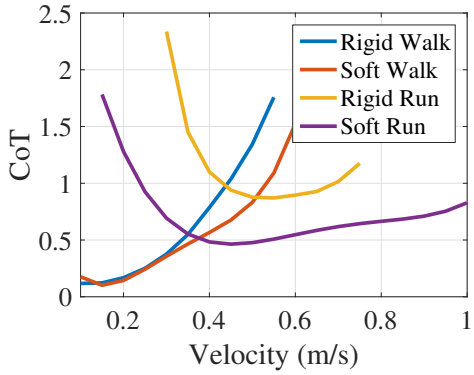

Figure 6 Comparison of the best robot performance in case of soft and rigid actuation for both the walk and run tasks. The curves report the minimum CoT results obtained over all the considered values of f_h.

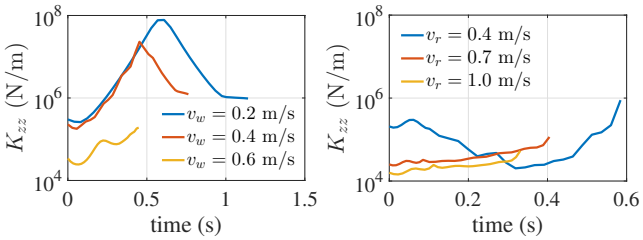

(a) (b)

Figure 7 Vertical stiffness analysis of the stance leg at $f_h = 0.01$ m, for different values of the forward speed, respectively in case of (a) walking and (b) running motion.

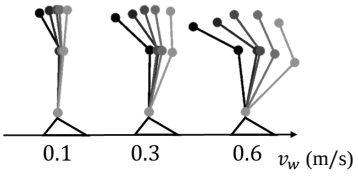

Figure 8 Walking: stance leg pose over time for different values of the forward speed v_w.

of this configuration variation, K_{zz} decreases as the forward speed increases. A similar trend can be observed also in running, see Figure 7(b). It is worth highlighting how the order of magnitude of the vertical stiffness in case of running is considerably lower compared to that obtained for low-speed walking. From these results it can be concluded that the more dynamic the task the more compliant is the optimal behaviour of the stance leg.

4 CONCLUSIONS

In this work, numerical optimal control was applied to obtain periodic walking and running gaits for a planar bipedal robot in case of rigid and soft actuation. Reference stiffness values for the Series Elastic Actuators (SEAs) were also optimised. The problem was stated as an optimal control one, so as to minimize the Cost of Transport (CoT) while constraining the motion feasibility, within actuation limits. The results showed the CoT sensitivity to forward speed and swing foot height. As regards the actuation type, a sensibly better performance of SEAs compared to rigid actuators could be observed in terms of CoT: specifically, in case of walking, the energy saving obtained by employing series elastic instead of rigid actuators increases as the forward speed increases (the soft system can save up to 38% of the CoT as compared to the rigid one at speed 0.55 m/s), whereas in case of running the soft actuation allows a considerably lower CoT over the whole considered forward speed range. Indeed, our results suggest that the more dynamic the task the more the elastic elements can be exploited to reduce energy consumption.

This observation was also confirmed by the analysis of the vertical Cartesian stiffness of the stance leg, which decreases as the forward speed increases.
Future work will be devoted to identify the joints whose compliance is particularly beneficial for locomotion. In addition, since the framework employed in this analysis is also suitable for investigating systems in which the stiffness of the actuators can vary over time, our next efforts will be aimed at assessing the possible advantages of employing Variable Stiffness Actuators (VSAs) in bipedal locomotion, also addressing whether the potential advantages are significant enough to make it worth dealing with the higher complexity of such actuators as compared to SEAs.

5 ACKNOWLEDGEMENTS

This work was supported by the European Commission via Grant No. 611832 "Walk-Man" within the FP7-ICT-2013-10 program.

REFERENCES

[1] Kim, S., Laschi, C., and Trimmer, B., "Soft robotics: a bioinspired evolution in robotics," *Trends in biotechnology*, vol. 31, no. 5, pp. 287–294, 2013.

[2] Rus, D. and Tolley, M. T., "Design, fabrication and control of soft robots," *Nature*, vol. 521, no. 7553, pp. 467–475, 2015.

[3] Ham, R., Sugar, T., Vanderborght, B., Hollander, K., and Lefeber, D., "Compliant actuator designs," *IEEE Robotics & Automation Magazine*, vol. 3, no. 16, pp. 81–94, 2009.

[4] Uemura, M. and Kawamura, S., "Resonance-based motion control method for multi-joint robot through combining stiffness adaptation and iterative learning control," in *Robotics and Automation (ICRA), 2009 IEEE International Conference on*, IEEE, 2009.

[5] Velasco, A., Gasparri, G. M., Garabini, M., Malagia, L., Salaris, P., and Bicchi, A., "Soft-actuators in cyclic motion: Analytical optimization of stiffness and pre-load," in *Humanoid Robots (HUMANOIDS), 2013 IEEE-RAS 13th International Conference on*, pp. 354–361, IEEE, 2013.

[6] Hof, A., Geelen, B., and Van den Berg, J., "Calf muscle moment, work and efficiency in level walking; role of series elasticity," *Journal of biomechanics*, vol. 16, no. 7, pp. 523–537, 1983.

[7] Cavagna, G. A., Heglund, N. C., and Taylor, C. R., "Mechanical work in terrestrial locomotion: two basic mechanisms for minimizing energy expenditure," *American Journal of Physiology-Regulatory, Integrative and Comparative Physiology*, vol. 233, no. 5, pp. R243–R261, 1977.

[8] Geyer, H., Seyfarth, A., and Blickhan, R., "Compliant leg behaviour explains basic dynamics of walking and running," *Proceedings of the Royal Society of London B: Biological Sciences*, vol. 273, no. 1603, pp. 2861–2867, 2006.

[9] Vanderborght, B., Verrelst, B., Van Ham, R., Van Damme, M., Lefeber, D., Duran, B. M. Y., and Beyl, P., "Exploiting natural dynamics to reduce energy consumption by controlling the compliance of soft actuators," *The International Journal of Robotics Research*, vol. 25, no. 4, pp. 343–358, 2006.

[10] WALKMAN,. `https://www.walk-man.eu`.

[11] Hopkins, M. A., Griffin, R. J., Leonessa, A., Lattimer, B. Y., and Furukawa, T., "Design of a compliant bipedal walking controller for the darpa robotics challenge," in *Humanoid Robots (HUMANOIDS), 2015 IEEE-RAS 15th International Conference on*, pp. 831–837, IEEE, 2015.

[12] Ackerman, E., "Durus: Sri's ultra-efficient walking humanoid robot," *IEEE SPECTRUM-Electronic source*, vol. 16, 2015.

[13] Vallery, H., Ekkelenkamp, R., Van Der Kooij, H., and Buss, M., "Passive and accurate torque control of series elastic actuators," in *Intelligent Robots and Systems, 2007. IROS 2007. IEEE/RSJ International Conference on*, pp. 3534–3538, IEEE, 2007.

[14] Srinivasan, M. and Ruina, A., "Computer optimization of a minimal biped model discovers walking and running," *Nature*, vol. 439, no. 7072, pp. 72–75, 2006.

[15] Schultz, G. and Mombaur, K., "Modeling and optimal control of human-like running," *IEEE/ASME Transactions on mechatronics*, vol. 15, no. 5, pp. 783–792, 2010.

[16] Schauß, T., Scheint, M., Sobotka, M., Seiberl, W., and Buss, M., "Effects of compliant ankles on bipedal locomotion," in *Robotics and Automation (ICRA), 2009. IEEE International Conference on*, pp. 2761–2766, IEEE, 2009.

[17] Werner, A., Lampariello, R., and Ott, C., "Trajectory optimization for walking robots with series elastic actuators," in *Decision and Control (CDC), 2014 IEEE 53rd Annual Conference on*, pp. 2964–2970, IEEE, 2014.

[18] Docquier, N., Poncelet, A., Fisette, P., and others,, "Robotran: a powerful symbolic generator of multibody models," *Mech. Sci*, vol. 4, no. 1, pp. 199–219, 2013.

[19] Andersson, J., *A General-Purpose Software Framework for Dynamic Optimization*. PhD thesis, Arenberg Doctoral School, KU Leuven, Belgium, 2013.

[20] Wächter, A. and Biegler, L. T., "On the implementation of an interior-point filter line-search algorithm for large-scale nonlinear programming," *Mathematical Programming*, vol. 106, no. 1, pp. 25–57, 2006.

[21] Buondonno, G., Carpentier, J., Saurel, G., Mansard, N., De Luca, A., and Laumond, J.-P., "Actuator design of compliant walkers via optimal control," in *2017 IEEE/RSJ International Conference on Intelligent Robots and Systems (IROS)*, pp. 705–711, IEEE, 2017.

[22] Ramezani, A., Hurst, J. W., Hamed, K. A., and Grizzle, J. W., "Performance analysis and feedback control of atrias, a three-dimensional bipedal robot," *Journal of Dynamic Systems, Measurement, and Control*, vol. 136, no. 2, p. 021012, 2014.

[23] Xi, W., Yesilevskiy, Y., and Remy, C. D., "Selecting gaits for economical locomotion of legged robots," *The International Journal of Robotics Research*, vol. 35, no. 9, pp. 1140–1154, 2016.

[24] Pratt, G. and Williamson, M. M., "Series elastic actuators," in *Intelligent Robots and Systems 95.'Human Robot Interaction and Cooperative Robots', Proceedings. 1995 IEEE/RSJ International Conference on*, vol. 1, pp. 399–406, IEEE, 1995.

[25] Spong, M. W., "Modeling and control of elastic joint robots," *Journal of dynamic systems, measurement, and control*, vol. 109, no. 4, pp. 310–319, 1987.

[26] Morris, B. and Grizzle, J., "Hybrid invariance in bipedal robots with series compliant actuators," in *Decision and Control, 2006 45th IEEE Conference on*, pp. 4793–4800, IEEE, 2006.

[27] Tucker, V. A., "The energetic cost of moving about: walking and running are extremely inefficient forms of locomotion. much greater efficiency is achieved by birds, fish—and bicyclists," *American Scientist*, vol. 63, no. 4, pp. 413–419, 1975.

[28] Sternberg, J., Gros, S., Houska, B., and Diehl, M., "Approximate robust optimal control of periodic systems with invariants and high-index differential algebraic systems," *IFAC Proceedings Volumes*, vol. 45, no. 13, pp. 690–695, 2012.

[29] Betts, J. T., *Practical methods for optimal control and estimation using nonlinear programming*. SIAM, 2nd ed., 2010.

[30] Della Santina, C., Piazza, C., Gasparri, G. M., Bonilla, M., Catalano, M., Garabini, M., Grioli, G., and Bicchi, A., "An open platform to fast-prototype articulated soft robots," *IEEE Robotics & Automation Magazine*, vol. 1070, no. 9932/17, 2017.

[31] Kuo, A. D., "A simple model of bipedal walking predicts the preferred speed–step length relationship," *Journal of biomechanical engineering*, vol. 123, no. 3, pp. 264–269, 2001.

[32] Hoyt, D. F., Wickler, S. J., and Cogger, E. A., "Time of contact and step length: the effect of limb length, running speed, load carrying and incline," *Journal of Experimental Biology*, vol. 203, no. 2, pp. 221–227, 2000.

[33] Albu-Schäffer, A., Fischer, M., Schreiber, G., Schoeppe, F., and Hirzinger, G., "Soft robotics: what cartesian stiffness can obtain with passively compliant, uncoupled joints?," in *Intelligent Robots and Systems (IROS), 2004 IEEE/RSJ International Conference on*, vol. 4, pp. 3295–3301, IEEE.